

**Pushing the boundaries
of chemistry?
It takes
#HumanChemistry**

Make your curiosity and talent as a chemist matter to the world with a specialty chemicals leader. Together, we combine cutting-edge science with engineering expertise to create solutions that answer real-world problems. Find out how our approach to technology creates more opportunities for growth, and see what chemistry can do for you at:

evonik.com/career

 **EVONIK**
Leading Beyond Chemistry

Reversible Photothermal Modulation of Electrical Activity of Excitable Cells using Polydopamine Nanoparticles

Hamed Gholami Derami, Prashant Gupta, Kuo-Chan Weng, Anushree Seth, Rohit Gupta, Jonathan R. Silva, Baranidharan Raman,* and Srikanth Singamaneni*

Advances in the design and synthesis of nanomaterials with desired biophysicochemical properties can be harnessed to develop non-invasive neuromodulation technologies. Here, the reversible modulation of the electrical activity of neurons and cardiomyocytes is demonstrated using polydopamine (PDA) nanoparticles as photothermal nanotransducers. In addition to their broad light absorption and excellent photothermal activity, PDA nanoparticles are highly biocompatible and biodegradable, making them excellent candidates for both in vitro and in vivo applications. The modulation of the activity (i.e., spike rate of the neurons and beating rate of cardiomyocytes) of excitable cells can be finely controlled by varying the excitation power density and irradiation duration. Under optimal conditions, reversible suppression ($\approx 100\%$) of neural activity and reversible enhancement (two-fold) in the beating rate of cardiomyocytes is demonstrated. To improve the ease of interfacing of photothermal transducers with these excitable cells and enable spatial localization of the photothermal stimulus, a collagen/PDA nanoparticle foam is realized, which can be used as an “add-on patch” for photothermal stimulation. The non-genetic optical neuromodulation approach using biocompatible and biodegradable nanoparticles represents a minimally invasive method for controlling the activity of excitable cells with potential applications in nano-neuroscience and engineering.

1. Introduction

Controlling a selective population of neurons to understand and establish a causal link between the neural activity and overall behavioral outcomes is a grand challenge in systems neuroscience. Harnessing the unique properties of matter at

Dr. H. Gholami Derami, P. Gupta, Dr. A. Seth, R. Gupta,
Prof. S. Singamaneni
Department of Mechanical Engineering and Materials Science
Institute of Materials Science and Engineering
Washington University in St. Louis
St. Louis, MO 63130, USA
E-mail: singamaneni@wustl.edu
Dr. K.-C. Weng, Prof. J. R. Silva, Prof. B. Raman
Department of Biomedical Engineering
Washington University in St. Louis
St. Louis, MO 63130, USA
E-mail: barani@wustl.edu

The ORCID identification number(s) for the author(s) of this article can be found under <https://doi.org/10.1002/adma.202008809>.

DOI: 10.1002/adma.202008809

the nanoscale to tackle this grand challenge has received increased attention over the past few years.^[1] Among the many methods that aim to modulate the biological processes, a particularly attractive method is photoregulation, a process in which light is utilized as an external stimulus.^[2] Since cells by themselves are not sensitive to photostimulation, insertion of light-sensitive ion channels and subsequent stimulation of these ion channels for selective neural control (i.e., optogenetics), has become an increasingly popular and staple tool for numerous investigations.^[3] While optogenetic techniques are promising and have revolutionized basic research aimed at understanding the computational and behavioral role of several different neural populations, there are still several limitations associated with these techniques that remain to be addressed.^[4] These include: i) the ability to excite neurons that are embedded deep in the tissue; ii) the ability to be widely used in different model organisms with or without a rich repertoire of genetic tools; iii) graded control of neurons; iv) the ability to control

different subset of neurons in a concurrent fashion; v) reversibility of the proposed approaches to return the controlled neurons to their original configuration; and, more importantly, vi) feasibility of developing a non-invasive approach. To address some of these shortcomings, the use of nanomaterials for non-genetic electrical and thermal stimulation were explored and tested successfully in recent years.^[5] Among these, photothermal methods have shown great promise and versatility in stimulating neuronal cells.^[6]

It has been reported that the absorption of the infrared (IR) light by water, converting it to thermal energy reversibly alters the electrical capacitance^[7] and therefore the excitability of nerve cells. However, direct IR stimulation is a non-specific approach that excites (or inhibits) many neurons in the area where optical illumination targets. The use of thermal energy as a stimulus to activate neurons could be highly localized to avoid global effects on neuronal firing and their behavior. Plasmonic nanostructures such as gold nanorods (AuNRs), which serve as locoregional photothermal transducers, have been employed to modulate (inhibit/stimulate) neural activity in vitro using near-IR (NIR) light.^[6a,c,h,i,8] Radio-frequency magnetic-field based

heating of magnetic nanoparticles has also been demonstrated to be effective in thermal activation of ion channels and triggering action potentials in cultured neurons.^[9] Magnetic nanoparticles were also used to target the motor cortex of moving mice and modulate its movement through magnetothermal stimulation.^[6c] Among various nanomaterials that could transform light energy to heat, polydopamine (PDA) nanoparticles are a particularly promising candidate for neuronal modulation due to their excellent photothermal properties, biocompatibility, biodegradability, and facile surface functionalization.^[10] PDA-based nanomaterials have been widely investigated as photothermal agents for photothermal cancer therapy.^[10b,11] Furthermore, due to their biocompatibility and superior interaction with cells, PDA-based nanomaterials have been shown to be promising candidates for neuronal interfacing.^[12]

Here, we explore the use of biocompatible and biodegradable PDA nanoparticles and a novel highly porous biofoam as photothermal agents to stimulate excitable cells such as neurons and cardiomyocytes with NIR light in a non-disruptive manner. This novel nanomaterial approach was utilized to localize the temperature around the excitable cells under 808 nm laser illumination. The change in the activity of neurons was monitored and quantified to understand the effect of different photothermal heating conditions. Electrical activity was measured for neurons and cardiomyocytes cultured on microelectrode array (MEA) to assess the ability of PDA nanoparticles and PDA-based foam to modulate the cell excitability. Series of quantitative analyses were performed to explain the effect of laser light intensity in the presence of PDA nanoparticles in modular and reversible control of the neuron and cardiomyocyte activity.

2. Results and Discussion

PDA nanoparticles are synthesized by oxidative self-polymerization of dopamine monomer in a water–ethanol–ammonium mixture at room temperature, using a previously reported method.^[13] Scanning electron microscopy (SEM) imaging and dynamic light scattering (DLS) measurement revealed the diameter of the PDA particles to be \approx 465 nm (Figure 1B,C). It has been recently reported that nanoparticle's interaction with neurons is solely dependent on its surface charge regardless of the shape, size, and composition.^[14] Negatively charged particles tend to adhere to the neuron cell membrane more efficiently than other particles. PDA, due to the presence of hydroxyl and amine functional groups on its surface, exhibits different surface charge under different pH conditions, with an isoelectric point at 3.3.^[15] Under physiological conditions (pH = 7.4), the zeta potential of PDA was measured to be -30.6 ± 0.3 mV (Figure S1, Supporting Information). PDA particles exhibited broad optical absorption ranging from 400 to 800 nm with a peak around 500 nm (Figure 1D). PDA nanoparticles exhibit excellent biocompatibility and biodegradability and provide high photothermal conversion efficiency and have been used as contrast agents for photothermal therapy.^[11a] Although the PDA NP optical absorption is higher at lower wavelength, NIR laser (808 nm wavelength) was used for photothermal stimulation owing to the low optical absorption of soft biological tissues in the NIR region (\approx 650–900 nm) compared to visible part

of the electromagnetic spectrum.^[16] NIR laser employed here confines the heat to the proximity of the photothermal nanoparticles, thus enabling locoregional neuromodulation. Under 808 nm laser irradiation (power density of 14 mW mm^{-2}), PDA particle suspension temperature increased with an increase in the concentration of the nanoparticles. For a concentration of $400 \mu\text{g mL}^{-1}$, the temperature increased by 25°C within 4 min, although the cell experiments are not conducted for this long period to prevent cell death (Figure 1E). It is worth noting that smaller changes in temperature ($\pm 5^\circ\text{C}$) as would be desirable for controlling cell excitability can be achieved within a few seconds. The magnitude of temperature rise under NIR laser irradiation can be controlled by tuning the power density of the laser, which is critical to avoid photothermally induced cell death (Figure 1F,G). Considering that the light absorption of cells and soft tissues in the NIR range is significantly lower compared to that in the visible part of the electromagnetic spectrum, 808 nm laser employed here confines the heat to the proximity of the photothermal nanoparticles, thus enabling locoregional neuromodulation.^[16]

To study the effect of nanoheating on the neuron viability, primary hippocampal neurons from prenatal rat were cultured on a substrate pre-coated with polyethylenimine (PEI) and laminin, sequentially. After 14 days in vitro, the neurons were immunolabeled for β -tubulin (III), which indicates good adhesion of neuron cells to the substrate and its long-term viability (Figure 2A).^[6c] The effect of photothermal heating on the viability of cultured neurons was examined by incubating them with PDA NPs and applying NIR light (Figure 2D). When irradiated with 808 nm laser at a power density of 14 mW mm^{-2} in the presence of PDA NP for 1, 2, and 5 min, no noticeable change in the viability of the neurons compared to the control groups was observed. The viability of neurons subjected to laser with and without PDA NP remained above 90%, indicating that the photothermal stimulation can be employed to modulate neuronal activity without inducing cell death.

To investigate the effect of photothermal heating on neurons activity, hippocampal neurons were cultured on MEAs and extracellular activity of neurons was recorded with and without PDA treatment and NIR stimulation (Figure 2B). Neurons cultured on MEA formed a dense network of neurites around titanium nitride (TiN) recording electrodes (Figure 2C). To ensure that the activity of the cultured neurons is stable and does not change over time, extracellular activity was recorded for 30 min without PDA treatment and NIR stimulation (Figure S2, Supporting Information). The overlaid waveform of cultured neurons exhibited stable activity without any significant change in the spike shape or amplitude over the entire recording duration (Figure 2E). Before stimulating the neurons with NIR laser in presence of PDA, the effect of PDA treatment on neurons baseline activity was examined (Figure 2F). Upon adherence of PDA nanoparticles to the plasma membrane of neurons, the mean spike rate of the neurons increased. This is possibly because the negatively charged PDA NPs induce a depolarization of the membrane potential by providing negative charge extracellularly to cause increased firing.^[14]

Following the formation of a complete network and reaching a stable spontaneous activity (\approx 14 days in vitro (DIV)), the neurons cultured on the MEAs were treated with PDA NPs

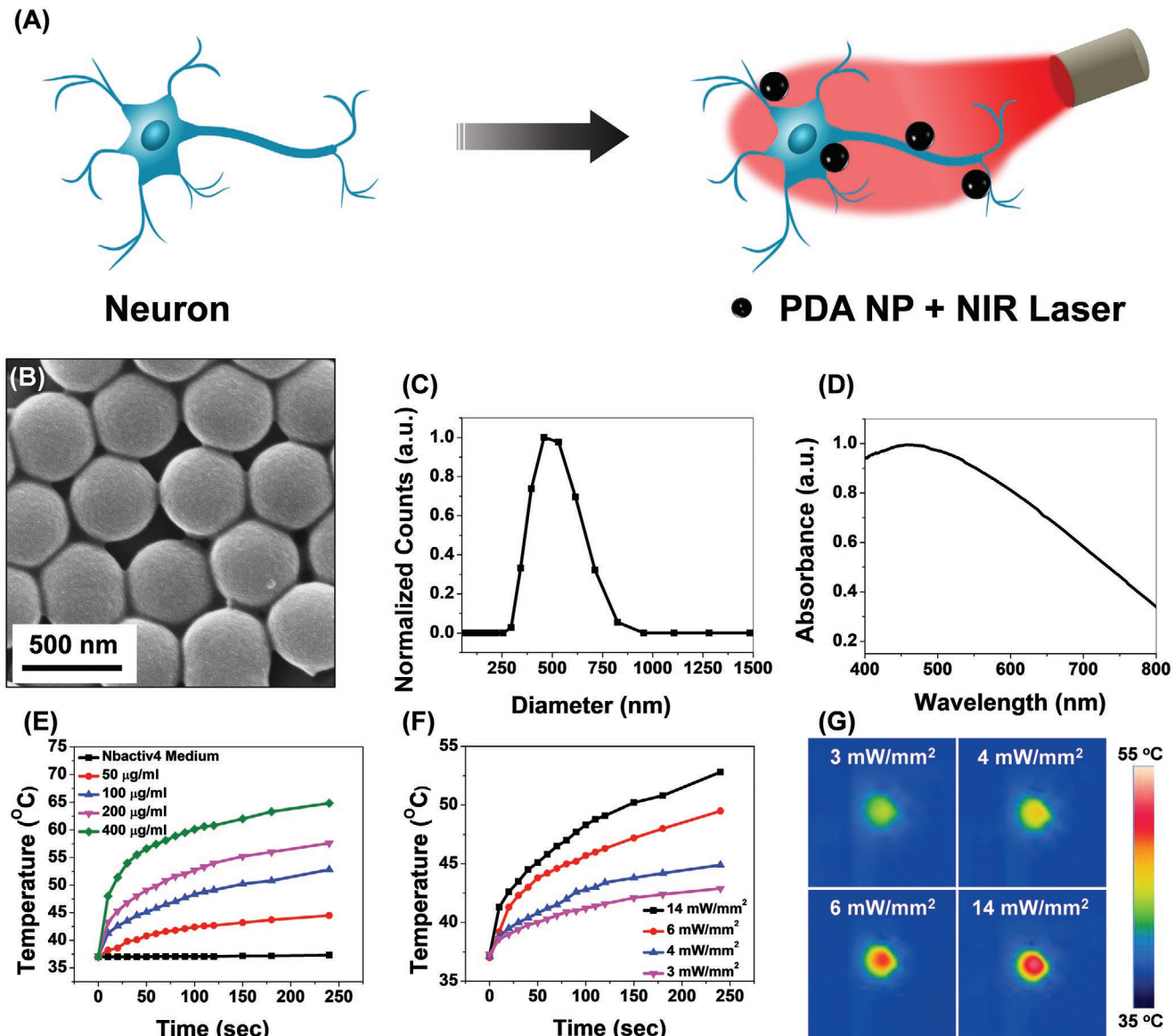


Figure 1. A) Schematic illustration of PDA-nanoparticles-mediated photothermal stimulation of neurons. PDA nanoparticles (PDA NPs) localized on the neuron modulate the neural activity through photothermal conversion of NIR light. B) SEM image, C) DLS measurement and D) absorption spectra of PDA NPs. E) Temperature changes in PDA NP solution with different concentrations at 14 mW mm^{-2} laser power density. F) Temperature changes in $100 \mu\text{g mL}^{-1}$ solution of PDA NP at different laser power densities and G) corresponding IR camera images of the PDA NP solution at the end of the laser illumination period.

($100 \mu\text{g mL}^{-1}$ final concentration) and incubated overnight. The PDA NPs adhered to neurons and the substrate and the rest of them gradually settled down and created a bed of particles on the cells and neurites which resulted in a particle-free solution before the activity recording and photothermal stimulation (Figure S3, Supporting Information). The cross-section TEM images of the neurons incubated with PDA NP did not reveal any internalization of the nanoparticles.^[17] The PDA-NP-treated neurons were subjected to repeated irradiation of 808 nm laser at different power densities for different stimulation duration (10, 20, and 30 s) in a back-to-back pulsatile fashion. The extracellular activity of the neurons was recorded before, during, and after the photothermal treatment (Figure 3A). It is worth

noting that TiN electrodes transmit $\approx 50\%$ of the light at 800 nm wavelength (Figure S4, Supporting Information). The extracellular signal recorded by each of these electrodes corresponds to a group of neurons on and around the electrodes that are irradiated by the NIR laser.

As can be noted, the neurons had spontaneous activity before any photostimulation. During the NIR irradiation, the number of action potentials fired reduced below spontaneous activity levels. Fewer spikes were detected for all power densities and for all durations tested (Figure 3A,C). The spike rate decreased monotonically with an increase in the NIR laser power density from 3 to 6 mW mm^{-2} (Figure 3B). At laser power density of 3 mW mm^{-2} , there was only 39% reduction in

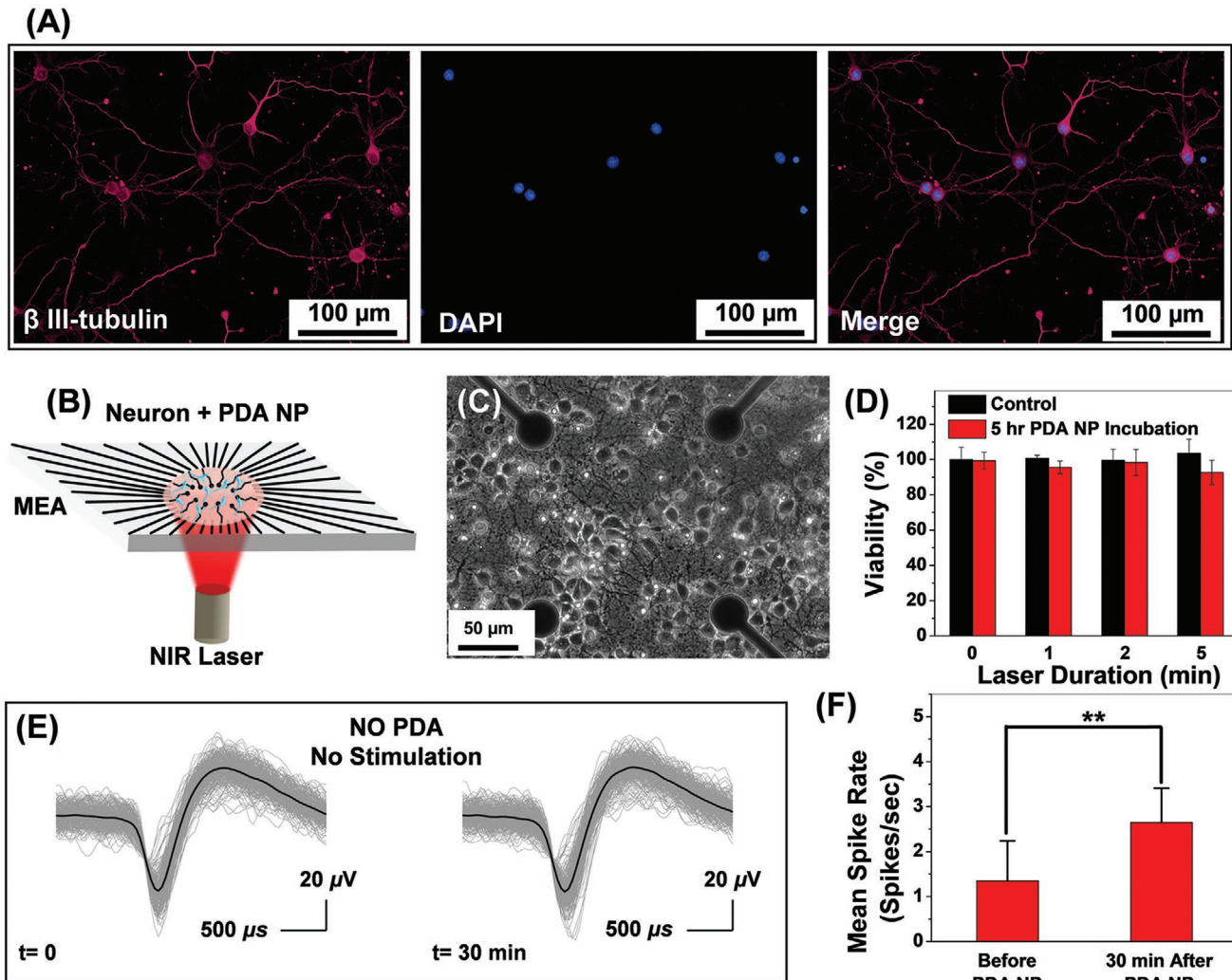


Figure 2. A) Fluorescence images of cultured hippocampal neurons after immunochemical staining of β -tubulin (III) (magenta) and nucleus (blue). B) Schematic illustration of the experimental setup with neurons cultured on a MEA and stimulated with NIR laser with and without PDA NP treatment. C) Phase-contrast image of the hippocampal neurons cultured on PEI-laminin-coated MEA with cell density of 1000 cells mm^{-2} . D) Cell viability of neurons subjected to 1, 2, and 5 min of NIR irradiation (14 mW mm^{-2}) without PDA NP (control) and with PDA NP ($100 \mu\text{g mL}^{-1}$ final concentration). The heat generated by NIR laser in the presence of PDA NP did not change the viability of the neurons compared to control sample (no PDA NP), indicating that it is safe to use PDA NP for photothermal treatment of neurons. E) Overlaid waveform of hippocampal neurons over half an hour time interval. Neurons were not treated with PDA NP and are not subject to any external stimulation. Spikes from 3 min recording with 256 spikes in each set (no change in mean spike rate). The black curve shows the mean value for each set and the gray curves illustrate individual spike waveforms. F) Effect of localization of PDA NP on neuron membrane on the mean spike rate of cultured neurons without NIR stimulation. Unpaired Two-samples t-test; $p = 0.0015$, $n = 21$, * $p < 0.05$, ** $p < 0.01$, *** $p < 0.001$, and **** $p < 0.0001$.

the spike rate compared to before NIR stimulation. The spike rate reduction reached 98% when laser power density increased to 6 mW mm^{-2} , suggesting an almost complete shutdown of neuron activity under these irradiation conditions. In comparison, neuron activity was recorded for cultures that were not treated with PDA NP but subjected to 808 nm laser irradiation (Figure S5, Supporting Information). The neuron activity did not change even under a significantly higher laser power density of 14 mW mm^{-2} (Figure S5A, Supporting Information). In the experiment without the presence of PDA particles, the mean spike rate measured before and during the laser irradiation did not change significantly. To investigate the effect of repeated laser stimulation, neuron activity was recorded for cultures

treated with PDA NP and over 10 repeats of 30 s NIR pulses at 6 mW mm^{-2} where almost complete activity shutdown was observed (Figure 3D and Figure S6, Supporting Information). The similarity in neural spike activity observed, summarized as a correlation matrix, during different photothermal stimulation periods/cycles/pulses showed that the evoked photothermal responses were highly similar. Photothermal treatment had a culture wide and universal effect of inhibiting neural spiking activity (Figure S6A, Supporting Information). The mean spike rate for PDA-NP-treated neurons was measured before the laser irradiation and after the finish of each cycle to reveal the possible permanent effect of photothermal treatment on neuron activity (Figure 3E). Although complete shutdown of

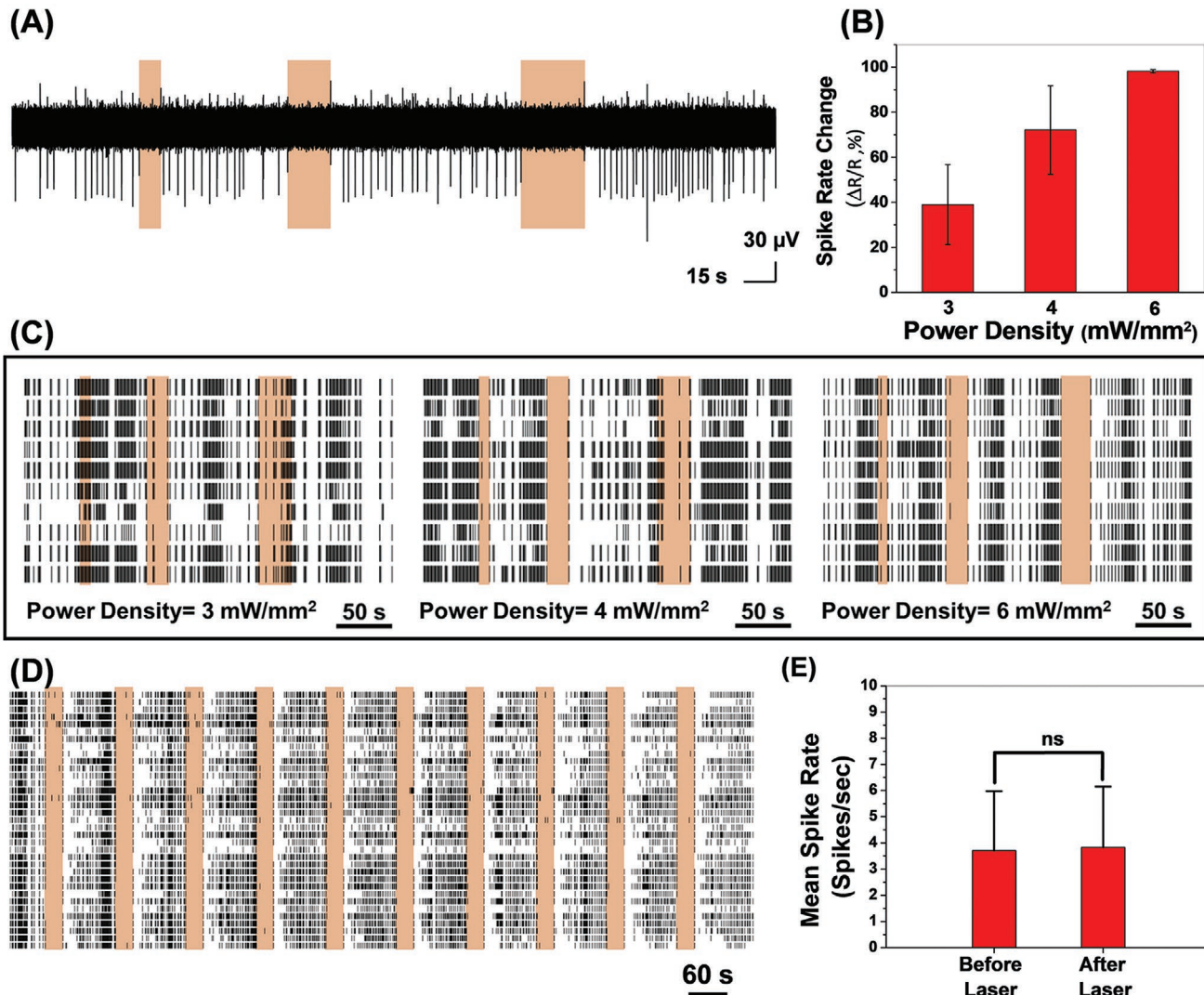


Figure 3. A) A single raw extracellular recording trace is shown. The colorbars identify three back-to-back NIR irradiation periods (10, 20, and 30 s laser irradiation at power density of 6 mW mm⁻²). B) Quantification of spike rate changes in (C) (effect of laser power density on spike rate change and inhibition of neuron activity). C) Spike rasters of neurons treated with PDA NP (100 μg mL⁻¹) with NIR irradiation at different power densities. Each row represents a single trial/cycle and each tick mark indicates an action potential fired. The ten rows show spontaneous neural firings and its modulation during NIR irradiation periods in ten different trials/cycles. D) Spike rasters of neurons treated with PDA NP (100 μg mL⁻¹) with NIR irradiation (power density of 6 mW mm⁻²) over 10 cycles of 30 s treatment. E) Mean spike rates of PDA-NP-treated neurons before and after NIR irradiation (data were collected for laser power density of 6 mW mm⁻² where neuron activities were completely suppressed during NIR irradiation, Unpaired Two-samples t-test; $p = 0.8866$, $n = 55$).

extracellular activity was noted during the laser irradiation (with PDA NP and at 6 mW mm⁻²), the mean spike rate after laser irradiation remained virtually identical to that observed before irradiation, indicating the reversible nature of the photothermal neuromodulation. Moreover, the spike shape and amplitude before and after the photothermal treatment did not show significant change for the same experiment indicating that neurons recovered their activity after photothermal treatment with no sign of temporary or permanent damage (Figure S7, Supporting Information).

Following the NIR irradiation period that resulted in complete inhibition of the neural activity, we noted that the neurons do not start firing immediately after stopping the irradiation

but recovered their baseline activity after a short time lag. We investigated the dependence of the neural activity recovery time on the laser power density and laser irradiation duration (Figure 4). By fixing the irradiation duration and increasing the laser power density from 3 to 6 mW mm⁻², the activity recovery time (the period between the end of NIR irradiation and the first spike for each electrode) increased significantly for all of the laser durations tested (Figure 4A). There was a small increase in the recovery time with an increase in the laser power density from 3 to 4 mW mm⁻². An increase in the laser power density from 4 to 6 mW mm⁻², resulted in a much larger increase in the lag time (Figure 4C). This is possibly due to the long cooling period required at higher laser power densities,

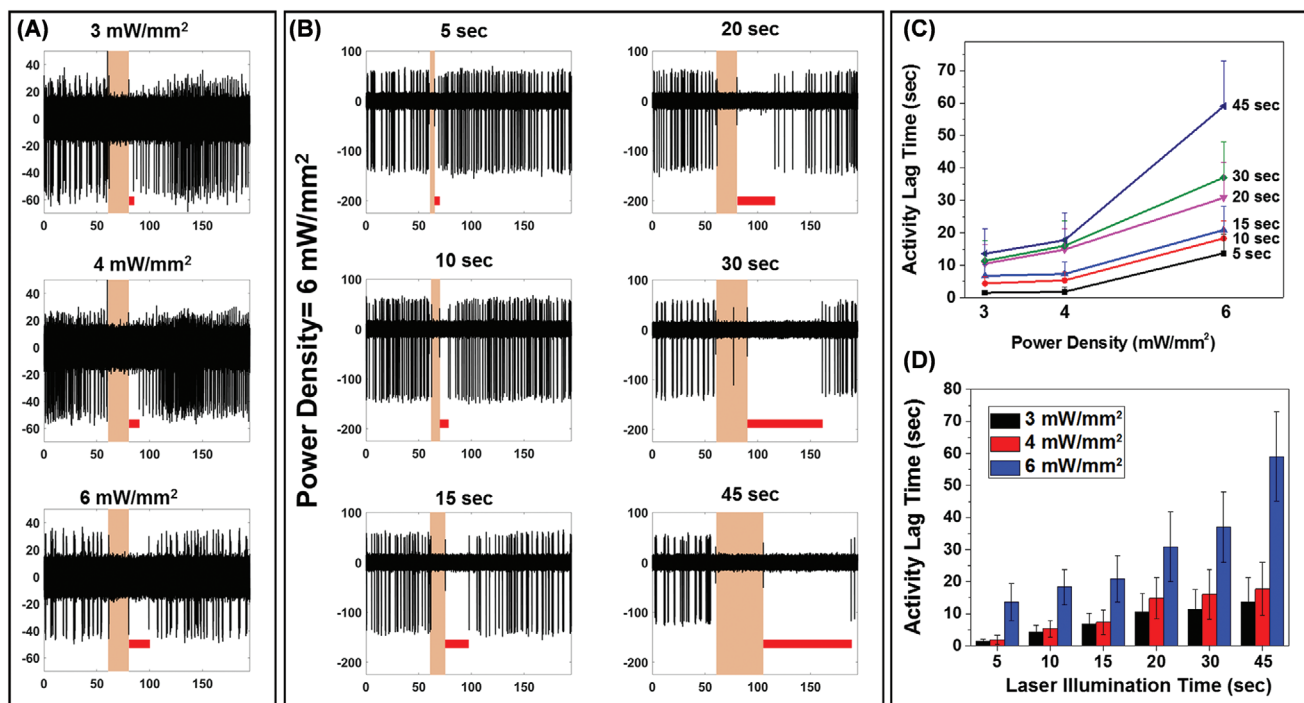


Figure 4. A) A single trace of extracellular recording from neurons treated with PDA NP is shown. The three individual panels reveal the effect on the spiking activities of PDA-NP-treated neurons before, during and after illumination at different laser power densities for a 20 s time window (color bar). The red lines show the activity lag time which is the amount of time it took after the laser illumination for the first spike to appear. B) Effect of laser duration on the activity lag time for PDA-NP-treated neurons (power density of 6 mW mm⁻²). C) Quantification of the effect of the laser duration on the activity lag time at different laser power densities. D) Quantification of the effect of the laser power density on the activity lag time at different laser duration times.

where the maximum temperature under laser irradiation is higher (Figure 1F). Alternately, stronger hyperpolarization during photostimulation period that at higher laser power densities could also result in longer recovery of resting membrane potential which could underlie similar monotonic increase in recovery time with response strength. In the case of fixed laser power density, an increase in the laser irradiation duration resulted in a monotonic increase in the activity lag time (Figure 4B). This increase in the activity lag time was more pronounced at the higher laser power density of 6 mW mm⁻² (Figure 4D). The particles on the substrate immediately adjacent to the neurons also contribute to the localized heating and delay the cooling process once the laser is turned off, thus causing a significant lag in the neuron activity recovery after each photothermal stimulation cycle. The tunable activity lag time with the laser power density and laser irradiation duration serves as an additional handle in light-based neuromodulation. On the other hand, specific targeting of the photothermal nanostructures to the neurons can minimize the non-specific adsorption of the nanostructures on the substrate and possibly minimize the activity lag time.

To test the generality of photothermal modulation on controlling cellular excitability, we have investigated the effect of PDA NPs and laser treatment on the electrical activity of cardiomyocytes. The iPSC-derived cardiomyocytes were differentiated and plated on the MEAs to assess the beating rates of cardiac tissues (Figure 5A). Without PDA NPs, upon laser stimulation, the beating rates of cardiac tissues increased only slightly (less

than 10%) and recovered to baseline rate once the laser irradiation is stopped (Figure 5B,C). Following the incubation of cardiomyocytes with PDA nanoparticles for 24 h, the beating rates under laser irradiation increased significantly compared to untreated cells subjected to laser irradiation (Figure 5D,E and Figure S8, Supporting Information). These results indicate the successful modulation of the electrical activity of the cardiomyocytes with photothermal nanostructures. To further understand the effect of localized heating on the tissue, PDA-NP-treated tissues were subjected to different laser power densities from 4 to 25 mW mm⁻² (Figure 5F–H and Figure S9, Supporting Information). With an increase in the laser power density from 4 to 14 mW mm⁻², the beating rate progressively increased and reached to \approx 1.8 times of the baseline activity (Figure 5F). For the highest laser power density (25 mW mm⁻²), the cardiomyocytes exhibited irreversible changes in the beating rate, indicating possible thermal toxicity (Figure S9, Supporting Information). The tissues not treated with PDA NPs exhibited only a small increase in the beating rate with a maximum increase of less than 10% at 14 mW mm⁻². These results demonstrate that the iPS-derived cardiac tissues showed a significant response to the localized nano-heating in the presence of PDA NPs with NIR laser irradiation. Also, the nature of the response changed from excitatory at lower laser power densities to inhibitory at laser power densities above 14 mW mm⁻² (Figure 5 and Figure S9, Supporting Information). The tunable modulation of the electrical activity of cardiomyocytes using PDA NPs could be harnessed for excitation and inhibition of

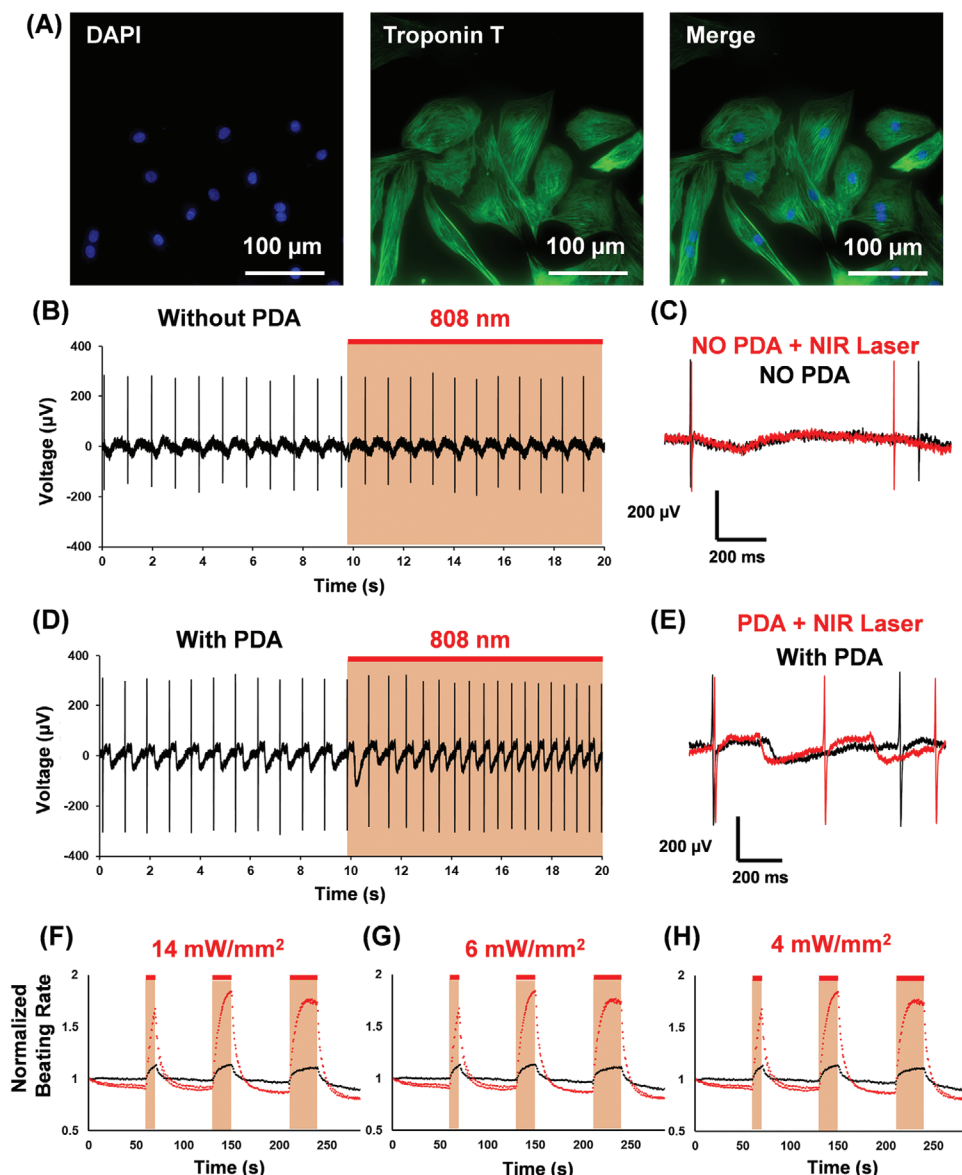


Figure 5. A) Immunofluorescence images of iPS-CMs counter-stained with DAPI (blue) and cardiac troponin T (green). B) The original trace of field potential recording of iPS-CMs from MEA system without PDA treatment. The laser power density was 14 mW mm⁻² and was turned on for 10 s as indicated using the color bar. C) The representative traces of field potential recordings of iPS-CMs without treatment with PDA nanoparticles before (black) and after (red) 808 nm laser excitation. D) The original trace of field potential recording of iPS-CMs from MEA system. The iPS-CMs were treated with PDA nanoparticles for 24 h and washed out before recording. The laser power density was 14 mW mm⁻² and was turned on for 10 s as indicated. E) The representative traces of field potential recordings of iPS-CMs treated with PDA nanoparticles before (black) and after (red) 808 nm laser excitation. F–H) The normalized beating rates of iPS-CMs before and after 808 nm laser excitation. At different laser power densities (14, 6, and 4 mW mm⁻²), the laser was turned on for 10, 20, and 30 s at the indicated time (the red lines show the data for experiments with PDA and laser, and black lines show data for only laser irradiation). The beating rates were determined by calculating the peak intervals of field potential recordings and normalized the rates at baseline.

cardiac activity is desired, simply by changing the laser power density.

The results discussed so far involve the incubation of the neurons (or cardiomyocytes) with colloidal PDA NP, which offers poor control over the distribution of the photothermally active nanostructures. To achieve better spatial control over photothermal stimulation and better photothermal performance, we have designed a highly porous 3D collagen foam

modified with PDA NPs as a conformal photothermal substrate (**Figure 6A**). Collagen foam is widely used in biomedical applications (e.g., wound dressing, tissue culture scaffolds) due to its highly porous structure and excellent biocompatibility.^[18] Pristine collagen foam is white (due to light scattering) and does not possess photothermal activity (Figure S10A, Supporting Information). When the collagen foam is exposed to a high concentration solution of PDA nanoparticles, within a few minutes,

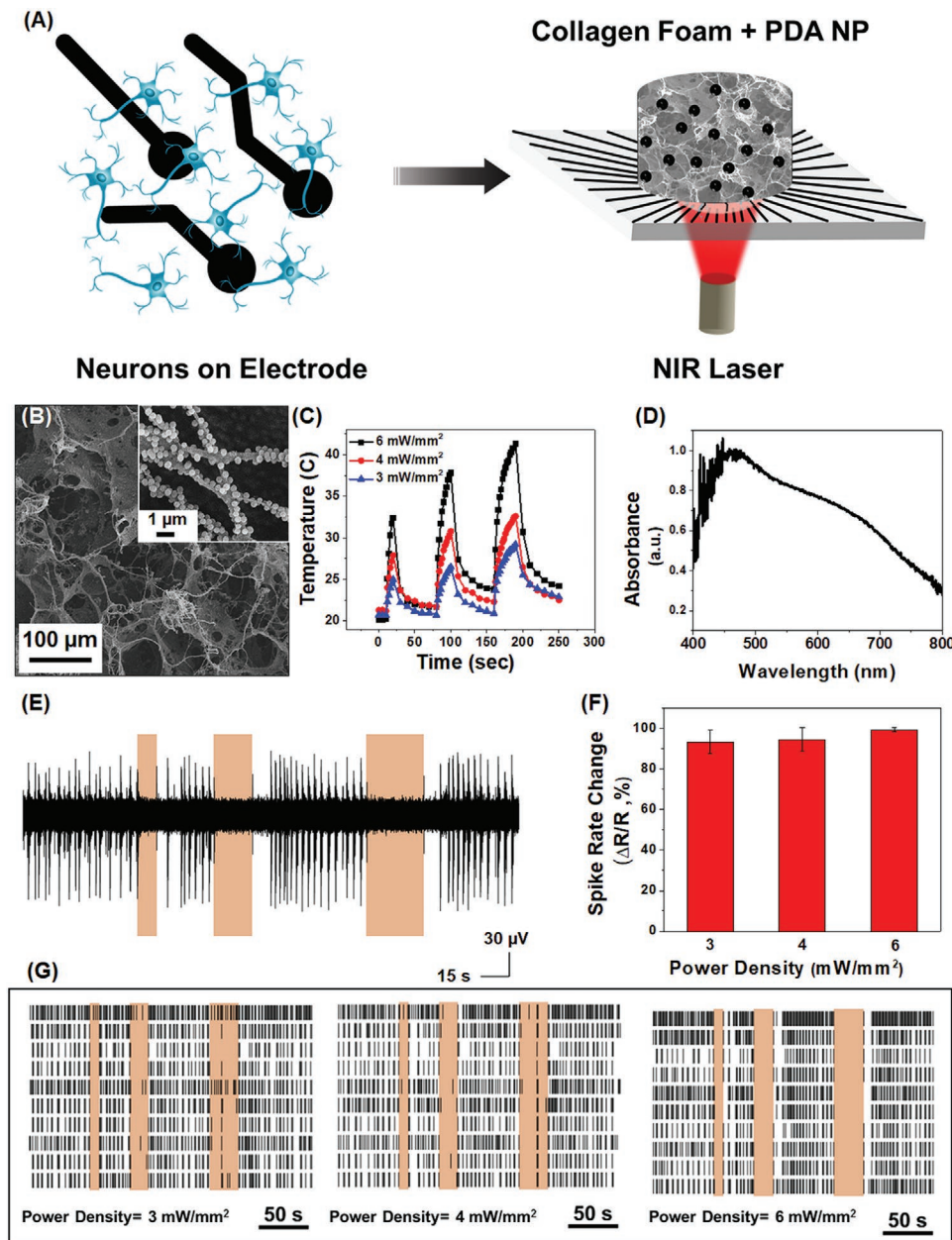


Figure 6. A) Schematic illustration of the experimental setup with neurons cultured on a MEA, collagen foam loaded with PDA NP placed on the culture and stimulated with NIR laser. B) SEM image (inset: higher-magnification SEM) and C) temperature changes of collagen foam + PDA NP in the wet state at different laser power densities. D) Absorption spectra of collagen foam loaded with PDA NP. E) A single extracellular recording trace illustrating neural spiking before, during and after three different NIR irradiation periods (10, 20, and 30 s laser irradiation at power density of 6 mW mm^{-2}). F) Quantification of spike rate changes in panel G (effect of laser power density on spike rate change and inhibition of neuron activity). G) Spike rasters of neurons with collagen foam loaded with PDA NP and NIR irradiation at different power densities. Similar plotting convention as in Figure 3C.

the collagen fibers are completely covered with PDA nanoparticles, as is indicated by its change of color from white to black (Figure S10B, Supporting Information). SEM images of the PDA-modified collagen foam (PDA/Collagen) reveal the high porosity and the PDA nanoparticles adsorbed on individual collagen fibers (Figure 6B). The PDA/collagen foam was found to be highly stable with no noticeable desorption of the PDA NP even under mechanical agitation. The absorbance spectrum of the PDA/collagen foam is similar to that of PDA NP solution

suggesting that photothermal efficiency for the foam should be similar to the PDA NPs (Figure 6D). In its dry state, the surface temperature of PDA/collagen foam increased by more than 100°C in just less than 10 s when irradiated by laser at a power density of 6 mW mm^{-2} (Figure S11, Supporting Information). Even at a much lower laser power density of 3 mW mm^{-2} , we noted a 60°C increase in the local surface temperature within the first 10 s. In wet state, the foam surface temperature rose by up to 12°C after 10 s and by up to 20°C after 30 s of irradiation

at a laser power density of 6 mW mm^{-2} (Figure 6C). The superior photothermal activity of the PDA/collagen foam compared to the high concentration of PDA NPs ($100 \mu\text{g mL}^{-1}$) stems from the highly dense adsorption of the PDA NPs on the collagen fibers and efficient light trapping within the foam due multiple reflections. In addition to the excellent photothermal properties, the highly porous PDA/collagen foam soaked in the cell culture medium can be applied as a conformal patch on cells and tissues.

To investigate the efficacy of PDA/collagen foam in photothermally modulating the neural activity, the foam was placed on the neurons cultured on the MEAs for 14 DIV, and after the neurons reached stable spontaneous activity. The neurons with PDA/collagen foam were subjected to repeated irradiation of 808 nm laser at different power densities for different stimulation durations (10, 20, and 30 s). The extracellular activity of the neurons was recorded during the photothermal treatment and it is evident that spiking activity during the photothermal stimulation is reduced drastically (Figure 6E,F). The quantitative measurement of the changes in the spike rate showed that at all the power densities tested, the neuron activity suppression was above 90% (Figure 6G). In comparison, at the same power density of 3 mW mm^{-2} , photothermal treatment of neurons treated with colloidal PDA NP resulted in only a 39% reduction in neuron activity. Moreover, when the power density was increased to 15 mW mm^{-2} , PDA/collagen foam resulted in permanent damage to cells, and the activity suppression was not reversible. This superior photothermal performance of the PDA/collagen compared to colloidal PDA NP allows the utilization of lower power light sources (e.g., near-IR LEDs) instead of laser for modulating the neural activity. Furthermore, this PDA/collagen 3D foam could be easily applied as a patch on brain tissues and cardiac tissues for modulating the electrical activity in a facile manner.

3. Conclusions

We have demonstrated the reversible and graded control of the electrical activity of excitable cells using PDA nanoparticles as biocompatible and biodegradable photothermal transducers. In the presence of PDA nanoparticles, the spike rate of neurons was significantly suppressed under NIR laser irradiation with a power density as low as 3 mW mm^{-2} . With a progressive increase in the laser power density, we observed a monotonic decrease in the spike rate. The activity recovery time was found to be dependent on irradiation power density and irradiation duration. The neural activity suppression and recovery were repeatable over 10 consecutive repetitions of laser irradiation, demonstrating the robustness of this non-invasive neuromodulation approach. In the presence of PDA nanoparticles, the beating rate of cardiomyocyte tissues progressively increased as the irradiation laser power density increased from 4 to 14 mW mm^{-2} . To improve the ease of interfacing the photothermal agents with neural cultures and brain tissues, we have designed and realized a 3D collagen/PDA nanoparticle foam and applied it on the cultured neurons as an “add-on” patch. The 3D foam demonstrated superior photothermal and neuromodulation performance compared to colloidal PDA

nanoparticles in that we observed more than 90 percent reduction in neuron activity even at laser power densities as low as 3 mW mm^{-2} . Compared to inorganic photothermal nanostructures (e.g., noble metal nanoparticles), PDA nanostructures are better suited for in vivo neuromodulation owing to their high biocompatibility and biodegradability. We believe that this novel material platform for non-invasive neuromodulation can be easily extended to other excitable cells both ex vivo and in vivo and serve as a valuable tool in nano-neuroengineering.

4. Experimental Section

Cell Culture: All procedures were approved by the Institutional Animal Care and Use Committee at Washington University in St. Louis. Hippocampal tissues were dissected from embryonic day 18 Sprague-Dawley rat brain (Charles River, USA). The tissues were transferred into Hibernate EB medium (HEB, BrainBits, USA) for further use. Cell dissociation solution was prepared by dissolving 6 mg papain (P4762, Sigma, USA) in 3 mL of Hibernate E-Ca (HE-Ca, BrainBits, USA). Hippocampal tissues were transferred to the cell dissociation solution and incubated at 30°C for 10 min. Dissociation solution was removed and HEB medium was added to the tissues, followed by trituration with fire-polished Pasteur pipette. Cell dispersion was centrifuged ($200 \times g$, 1 min) and the supernatant was removed, and the pellets were resuspended in NbActiv4 (BrainBits, USA). Substrates were pre-treated with poly(ethyleneimine) solution (0.1% in water, P3143, Sigma, USA) for 30 min followed by air drying. Before the cell seeding, substrates were treated with laminin solution ($20 \mu\text{g mL}^{-1}$ in NbActiv4 medium, L2020, Sigma, USA). After removing the extra laminin solution, cells were seeded at the density of $500\text{--}1000 \text{ cells mm}^{-2}$ and maintained in the NbActiv4 medium in a humidified incubator with $5\% \text{ CO}_2$ and 37°C condition. After 2 days, half of the medium was changed with fresh NbActiv4 medium and was regularly changed every 4 days.

For iPS-derived cardiomyocytes (iPS-CMs), the WTC-11-GCaMP6 from Bruce Conklin Lab in Gladstone Institute were used as the induced pluripotent stem cells (iPSC). The iPSCs were maintained in E8 medium (Thermo Fisher Scientific) on Matrigel-coated (Corning) tissue culture plate and passaged every four days. The protocols used to differentiate and purify iPS-derived cardiomyocytes (iPS-CMs) were through Wnt modulation and lactate purification that was previously described.^[19]

PDA Nanoparticle and Collagen/PDA Foam Preparation: All chemicals were purchased from Millipore Sigma, St. Louis, USA and used without further modification. PDA particles were synthesized by using a method described elsewhere.^[13] In a typical synthesis procedure of PDA nanoparticles, 252 mL of deionized (DI) water (resistivity $>18.2 \text{ M}\Omega \text{ cm}$) was mixed with 112 mL of ethanol in a 1000 mL glass container. Subsequently, 1.96 mL of aqueous solution of ammonia (28–30% NH₄OH) was introduced into the above water/ethanol mixture. After stirring for 30 min, the aqueous solution of dopamine hydrochloride (1.4 g in 28 mL) was added to the above solution. The reaction was left under gentle magnetic stirring for 24 h with no cap on the glass container. The PDA particles were collected by centrifugation (9000 rpm, 10 min) and washed with DI water three times and dispersed in water (320 mL).

To prepare the photothermally active 3D foam, a collagen film (HeliTAPE Collagen Wound Dressing, Miltex Instruments, USA) was soaked in water to create a hydrogel. The collagen hydrogel was then freeze-dried to achieve highly porous 3D foam. The collagen foam was soaked in the PDA NP solution (1 mg mL^{-1} in water) and left for 5 min with shaking followed by washing with water to remove the excess nanoparticles. The PDA-NP-loaded collagen foam was freeze-dried again to be used in the photothermal stimulation experiments.

Material Characterization: SEM images were obtained by using a JEOL JSM-7001 LVF Field Emission SEM. DLS and zeta potential measurements were performed using Malvern Zetasizer

(Nano ZS). Shimadzu UV-1800 spectrophotometer was employed for light-absorption measurements.

Photothermal Stimulation: A fiber optic NIR laser (808 nm) was used for a light source and the laser beam spot size and power density was controlled by its distance from the MEA (Multichannel Systems, Germany). Hippocampal neuronal networks were cultured on a MEA chip and incubated with PDA NPs overnight. The PDA-NP-treated neurons were then repeatedly irradiated with a NIR laser (808 nm) at different power densities and durations. A typical photothermal experiment lasts for 330 s, and the cells were illuminated with laser at different power densities for 10, 20, and 30 s. The laser on and off was controlled by a mechanical shutter. For repeatability experiment, cells were illuminated for 30 s with a power density of 6 mW mm⁻² followed by 90 s of no laser illumination for 10 cycles. The experiment for calculating the neuron activity recovery time after laser illumination was performed by recording the activity for 60 s followed by laser pulses with different durations and power densities followed by at least 90 s wait time, for a total of 210 s. Same experimental procedures were followed for cardiomyocytes.

Electrical Activity Recording: Neural recordings were obtained from neuronal cultures at the age of 14–18 DIV. Extracellular activity from cultured neurons were monitored using 60-channel TiN MEAs (MultiChannel Systems, diameter 30 μm, electrode spacing 200 μm, 500 nm thickness of Si₃N₄ insulator). Electrode signals were amplified and digitized with an in vitro MEA system (Multichannel systems, gain 1100, bandwidth 10–8 kHz, sampling frequency 25 kHz). The recorded signals were filtered with a 200 Hz digital high pass filter (Butterworth, second order), and spikes were detected by setting the threshold level at five times the standard deviation of background noise using vendor provided software (MC_Rack, MultiChannel Systems). Recording condition was maintained at 37 °C and 5% CO₂. Collected data were processed using MATLAB (MathWorks). For bulk heating experiments, the head stage temperature was adjusted to desired value and after 15 min of stabilization, the neuron activity recording was performed. To test the effect of PDA NP on neuron activity without laser stimulation, the extracellular activity of cultured neurons was recorded for 30 min before addition of PDA NP after which the culture was incubated with PDA NP solution (100 μg mL⁻¹ final concentration).

To record the field potential activities of iPS-CM, the iPS-CMs were suspended at 30 × 10⁶ cells mL⁻¹ and a 4 μL droplet was seeded on the recording area of MEA probe (60MEA200/10iR-Ti). The field potentials were recorded using MC_Rack software (Multichannel Systems) at 10000 Hz sampling rate with a 200 Hz digital high pass filter (Butterworth, second order). The data were converted to ABF format using MC_Data Tool (Multichannel Systems) and the field potentials were analyzed using Clampfit 10.7 (Molecular Devices) and MATLAB (MathWorks).

Cell Viability: Hippocampal neurons were cultured in pre-treated 96 well black plates at the density of 20,000 cells per well for 14 DIV and treated with PDA NPs at 100 μg mL⁻¹ final concentration. After 5 h incubation, they were subjected to 808 nm laser for 10 min at a power density of 14 mW mm⁻². After 24 h, MTS assay was performed as per manufacturer protocol.

Data Analysis: Recording channels whose average firing rate was larger than 0.1 spikes per second were selected as active channels and used for neural activity analysis. For the analysis of spontaneous activity, peri-event time histogram and raster plots were used with the NIR irradiation as an event. The spike rate reduction ($\Delta R/R$) with or without the NIR irradiation was calculated by the following equation: $\Delta R/R (\%) = [R(ON) - R(OFF)]/R(OFF)$, where $R(OFF)$ and $R(ON)$ indicate the average spike rate before and after the onset of NIR irradiation, respectively. $R(ON)$ covered the entire irradiation period (5–45 s), and $R(OFF)$ covers the 30 s window just before the onset of the irradiation. Note that plots in Figure 3B and 6F show absolute values. All statistics were performed with 5% one-sided significance level.

Immunostaining: Hippocampal neurons were fixed in 4% neutral buffered formalin in 1× PBS for 30 min at room temperature and washed with PBS three times. To permeabilize the cells, neurons were incubated

with 0.5% Triton X-100 in 1× PBS for 10 min at room temperature and washed with PBS three times. The nonspecific binding of antibodies was blocked by 6% bovine serum albumin (BSA, Sigma) in PBS for 30 min, and washed with PBS once. The biotinylated primary antibody (neuron-specific β-III tubulin antibody, 6 μg mL⁻¹ in 1.5% BSA, R&D systems MAB 1195) was added to the cells and incubated for 3 h at RT. After washing with PBS for three times, streptavidin-tagged fluorescent dye (IRDye 800CW Streptavidin, 50 ng mL⁻¹ in 1.5% BSA, LI-COR) were incubated with the cells for 30 min at RT. After washing with PBS for three times, DAPI solution (300 × 10⁻⁹ M in PBS, Sigma) was used for nucleus staining. Fluorescence images were obtained using a Lionheart FX Automated Microscope (BioTek, USA). The iPSC-derived cardiomyocytes were seeded on glass slide at day 30. The cells were fixed with 4% (v/v) paraformaldehyde for 30 min and stained with primary antibody TNNT2 (ab45923; Abcam) and secondary antibody Alexa Fluor 488 goat anti-rabbit IgG (A11008; Invitrogen) and nuclei counterstained by DAPI solution (1 μg mL⁻¹).

Supporting Information

Supporting Information is available from the Wiley Online Library or from the author.

Acknowledgements

The authors acknowledge support from Air Force Office of Scientific Research (#FA95501910394 (S.S. and B.R.)) and National Institutes of Health (R01-HL136553 (J.R.S.)). The authors thank Nano Research Facility (NRF) and Institute of Materials Science and Engineering at Washington University for providing access to electron microscopy facilities.

Conflict of Interest

The authors declare no conflict of interest.

Data Availability Statement

Research data are not shared.

Keywords

light-to-heat conversion, nano-neuro interfaces, neuromodulation, photothermal stimulation, polydopamine nanoparticles

Received: December 29, 2020

Revised: April 15, 2021

Published online: July 3, 2021

- [1] a) S. M. Won, E. Song, J. Zhao, J. Li, J. Rivnay, J. A. Rogers, *Adv. Mater.* **2018**, *30*, 1800534; b) J. Li, H. Duan, K. Pu, *Adv. Mater.* **2019**, *31*, 1901607; c) P. Fattah, G. Yang, G. Kim, M. R. Abidian, *Adv. Mater.* **2014**, *26*, 1846; d) Y. C. Jeong, H. E. Lee, A. Shin, D. G. Kim, K. J. Lee, D. Kim, *Adv. Mater.* **2020**, *32*, 1907522; e) N. Obidin, F. Tasnim, C. Dagdeviren, *Adv. Mater.* **2020**, *32*, 1901482.

- [2] J. Li, K. Pu, *Chem. Soc. Rev.* **2019**, *48*, 38.

- [3] a) E. S. Boyden, F. Zhang, E. Bamberg, G. Nagel, K. Deisseroth, *Nat. Neurosci.* **2005**, *8*, 1263; b) B. V. Zemelman, G. A. Lee, M. Ng, G. Miesenböck, *Neuron* **2002**, *33*, 15.
- [4] a) J. G. Bernstein, E. S. Boyden, *Trends Cognit. Sci.* **2011**, *15*, 592; b) K. Deisseroth, G. Feng, A. K. Majewska, G. Miesenböck, A. Ting, M. J. Schnitzer, *J. Neurosci.* **2006**, *26*, 10380; c) E. M. Callaway, R. Yuste, *Curr. Opin. Neurobiol.* **2002**, *12*, 587.
- [5] Y. Wang, L. Guo, *Front. Neurosci.* **2016**, *10*, 69.
- [6] a) S. Yoo, J.-H. Park, Y. Nam, *ACS Nano* **2018**, *13*, 544; b) S. K. Rastogi, R. Garg, M. G. Scopelliti, B. I. Pinto, J. E. Hartung, S. Kim, C. G. E. Murphey, N. Johnson, D. San Roman, F. Bezanilla, J. F. Cahoon, M. S. Gold, M. Chamanzar, T. Cohen-Karni, *Proc. Natl. Acad. Sci. U. S. A.* **2020**, *117*, 13339; c) S. Yoo, S. Hong, Y. Choi, J.-H. Park, Y. Nam, *ACS Nano* **2014**, *8*, 8040; d) J. L. Carvalho-de-Souza, J. S. Treger, B. Dang, S. B. H. Kent, D. R. Pepperberg, F. Bezanilla, *Neuron* **2015**, *86*, 207; e) R. Munshi, S. M. Qadri, Q. Zhang, I. C. Rubio, P. Del Pino, A. Pralle, *eLife* **2017**, *6*, e27069; f) H. Kang, G.-H. Lee, H. Jung, J. W. Lee, Y. Nam, *ACS Nano* **2018**, *12*, 1128; g) J. W. Lee, H. Jung, H. H. Cho, J. H. Lee, Y. Nam, *Biomaterials* **2018**, *153*, 59; h) K. Eom, J. Kim, J. M. Choi, T. Kang, J. W. Chang, K. M. Byun, S. B. Jun, S. J. Kim, *Small* **2014**, *10*, 3853; i) S. Yoo, R. Kim, J.-H. Park, Y. Nam, *ACS Nano* **2016**, *10*, 4274.
- [7] Mikhail G. Shapiro, Kazuaki Homma, Sebastian Villarreal, C.-P. Richter, F. Bezanilla, *Nat. Commun.* **2012**, *3*, 736.
- [8] J. Yong, K. Needham, W. G. A. Brown, B. A. Nayagam, S. L. McArthur, A. Yu, P. R. Stoddart, *Adv. Healthcare Mater.* **2014**, *3*, 1862.
- [9] a) J. Dobson, *Nat. Nanotechnol.* **2008**, *3*, 139; b) H. Huang, S. Delikanli, H. Zeng, D. M. Ferkey, A. Pralle, *Nat. Nanotechnol.* **2010**, *5*, 602.
- [10] a) R. Batul, T. Tamanna, A. Khaliq, A. Yu, *Biomater. Sci.* **2017**, *5*, 1204; b) A. Seth, H. Gholami Derami, P. Gupta, Z. Wang, P. Rathi, R. Gupta, T. Cao, J. J. Morrissey, S. Singamaneni, *ACS Appl. Mater. Interfaces* **2020**, *12*, 42499.
- [11] a) Y. Liu, K. Ai, J. Liu, M. Deng, Y. He, L. Lu, *Adv. Mater.* **2013**, *25*, 1353; b) D.-Y. Zhang, Y. Zheng, H. Zhang, J.-H. Sun, C.-P. Tan, L. He, W. Zhang, L.-N. Ji, Z.-W. Mao, *Adv. Sci.* **2018**, *5*, 1800581.
- [12] a) K. Kang, S. Lee, R. Kim, I. S. Choi, Y. Nam, *Angew. Chem.* **2012**, *124*, 13278; b) M. Battaglini, A. Marino, A. Carmignani, C. Tapeinos, V. Cauda, A. Ancona, N. Garino, V. Vighetto, G. La Rosa, E. Sinibaldi, *ACS Appl. Mater. Interfaces* **2020**, *12*, 35782; c) A. Golabchi, B. Wu, B. Cao, C. J. Bettinger, X. T. Cui, *Biomaterials* **2019**, *225*, 119519.
- [13] K. Ai, Y. Liu, C. Ruan, L. Lu, G. Lu, *Adv. Mater.* **2013**, *25*, 998.
- [14] S. Dante, A. Petrelli, E. M. Petrini, R. Marotta, A. Maccione, A. Alabastri, A. Quarta, F. De Donato, T. Rivasenga, A. Sathya, R. Cingolani, R. Proietti Zaccaria, L. Berdondini, A. Barberis, T. Pellegrino, *ACS Nano* **2017**, *11*, 6630.
- [15] H. Gholami Derami, Q. Jiang, D. Ghim, S. Cao, Y. J. Chandar, J. J. Morrissey, Y.-S. Jun, S. Singamaneni, *ACS Appl. Nano Mater.* **2019**, *2*, 1092.
- [16] a) R. Weissleder, *Nat. Biotechnol.* **2001**, *19*, 316; b) A. M. Smith, M. C. Mancini, S. Nie, *Nat. Nanotechnol.* **2009**, *4*, 710.
- [17] a) D. H. Jo, J. H. Kim, T. G. Lee, J. H. Kim, *Nanomed.: Nanotechnol. Biol. Med.* **2015**, *11*, 1603; b) Y. Wong, K. Markham, Z. P. Xu, M. Chen, G. Q. Lu, P. F. Bartlett, H. M. Cooper, *Biomaterials* **2010**, *31*, 8770.
- [18] a) B. Aslan, S. Guler, A. Tevlek, H. M. Aydin, *J. Biomed. Mater. Res., Part B* **2018**, *106*, 2157; b) S. J. Mackenzie, J. L. Yi, A. Singla, T. M. Russell, D. J. Osterhout, B. Calancie, *Muscle Nerve* **2018**, *57*, E78.
- [19] a) X. Lian, C. Hsiao, G. Wilson, K. Zhu, L. B. Hazeltine, S. M. Azarin, K. K. Raval, J. Zhang, T. J. Kamp, S. P. Palecek, *Proc. Natl. Acad. Sci. U. S. A.* **2012**, *109*, E1848; b) S. Tohyama, F. Hattori, M. Sano, T. Hishiki, Y. Nagahata, T. Matsuura, H. Hashimoto, T. Suzuki, H. Yamashita, Y. Satoh, *Cell Stem Cell* **2013**, *12*, 127.